Jurnal Mekanikal
June 2011, No. 32, 73 - 85

FLOW IMPROVEMENT USING CFD FOR PASSENGER CAR : BI AND UNI-DIRECTIONAL APPLICATION

Kannan M. Munisamy*, Norshah Hafeez Shuaib, Mohd. Zamri Yusoff and Savithry K. Thangaraju

College of Engineering,
Universiti Tenaga Nasional,
Jalan IKRAM-UNITEN, 43009,
Kajang, Selangor, Malaysia.

ABSTRACT

This paper presents experimental and Computational Fluids Dynamics (CFD) investigations of the flow in brake discs. Development of an experiment rig with basic measuring devices are detailed out and validated. The straight blade is improved with different blade configuration with same brake disc dimension. The three dimensional model is simulated in proprietary CFD software FLUENT™ and the mass flow through the ventilated blades are compared. From the simulations, it can be concluded that the improving the blade yields a great mass flow improvement which would improve the heat transfer performance but it constrained the disc to be uni-directional disc.

Keyword: *Ventilated brake disc, flow measurement, computational fluid dynamics (CFD), heat transfer.*

1.0 INTRODUCTION

Braking technology has improved tremendously throughout the twentieth century. In the last decade the requirement on the brake disc cooling is increased due to significant increase in vehicle speed, weight, and acceleration. Currently, following claims of higher cooling efficiency, the ventilated disc brake is fast becoming the state of the art in automotive braking system. Several works has been done to investigate the various aspects of performance of conventional and ventilated brake discs.

The earliest interest was shown by Newcomb and El-Sherbiny [1] on wet brakes on road to cool down the high temperature on the brake disc. An analytical solution for temperature rise during braking and some result from road testing of a heavy vehicle were presented. The application is recommended for heavy vehicles like buses and lorries. The authors also presented a general view about energy dissipation and energy saving possibilities during braking. Dow [2] and Moore [3] reported work on experimental rig development for the whole brake system rather than a single brake disc. They performed series of dynamometer braking experiment at British Railways to study the appearance of hot spots on wheels for a number of brake shoe materials. There were considerable

*Corresponding author's email: kannan@uniten.edu.my

experimental evidence to show that the thermo elastic interactive take place in both disc and on-tread railroad brakes. Yevtushenko and Ivanyk [4] have reported an analytical model to find the surface friction temperature which was validated with literature experimental data for railway and aircraft applications.

Laskaj and Murphy [5], in collaboration with The Ford Tickford Racing (FTR), studied the design of the cooling air ducting for disc brake of Glenn Seton's V8 racing car. The special brake pads made of titanium and ceramic need to be around 550°C to operate effectively. However in the real case the temperature was measured up to 750°C. They reported that, at high temperatures brake fading happens whereby the metal surface losses the strength and surface friction. The friction coefficient decreases with increasing temperature, leading to more force required to be applied from brake pads to brake disc. Thus, more energy is transferred to heat, compounding the problem. The aim of the study was to increase cooling of the brake disc, which can be done by increasing exit velocity of the ducting to the disc and increasing the surface area that the air blows. It is known that the two means will increase heat transfer rate. Harmand et. al. [6] studied the convective heat transfer properties for a rotor-stator system with rotor outer radius of 310mm. The flow structure between the rotor and the stator was analyzed by Particle Imaging Velocimetry (PIV) technique. Johnson et. al. [7] reported an interesting experimental work on flow visualization through ventilated brake disc using Particular Image Velocimetry (PIV). Inlet flow measurement shows significant misalignment due to the swirling entry of the flow. In the internal flow passage, large separation is found on the suction side surface. A study on the thermal gradient appearance on the surface of railway brake disc is done by Panier S., et. al. [8]. A full scale test bench with infrared camera measurement on the rubbing temperature during braking was built and classification of hot spots was observed. The author stated that hot spots classifications from the experiments are the actual phenomena in railway and aircraft disc brakes with reference to other previous publications.

Besides the studies on the flow and heat transfer properties of brake discs, extensive work is reported on the vibration and noise factor of the brake disc system (for example [9, 10, 11, 12, 13].

The aim of this paper is to report the development of the experimental rig for the investigation of flow in rotating brake disc and the subsequent CFD simulation for the purpose of comparison. Having validated the CFD models against the experimental data, the effect of blade tilting is investigated numerically.

2.0 BRAKE DISC SPECIMEN

The actual size of the brake disc used in a commercial passenger car is replicated in the current work. The prototype is made of aluminum due its lower cost of machining and stability in term of oxidization during storage. For the experimental rig, the straight (conventional) 36 blade brake disc design is used. The height and thickness of the blade are 10mm and 4mm respectively. The top view with blade design and dimension are shown in Figure 1. The analysis on the improved tiled angled blade is based on the specimen in Figure 2.

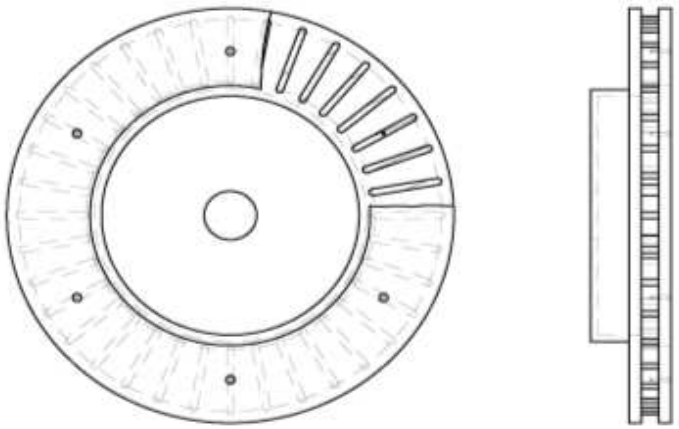

Figure 1: Top view of the straight blade ventilated brake disc

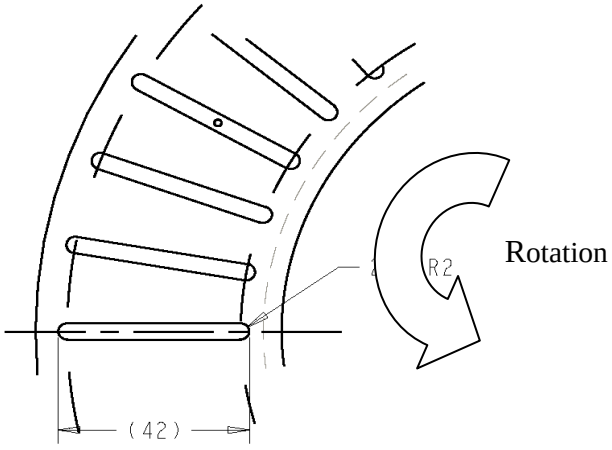

(a)

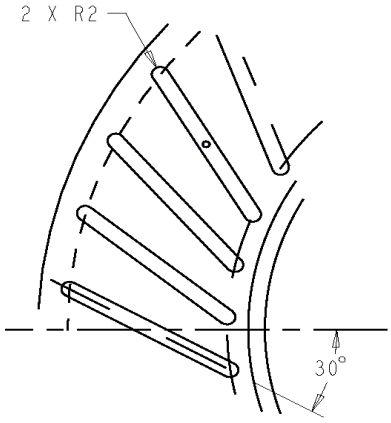

(b)

Figure 2 : Blade orientation configuration: a) 0° angle (baseline); b) 30° titled angle

3.0 EXPERIMENTAL RIG DESCRIPTION

The schematic of the experimental rig illustrated in Figure 3. As shown, to constraint the flow through the disc specimen, a specifically design brake disc casing is fabricated. In order to measure the air inflow velocity, an external flow circular ducting was built. Additional tapping is also made on the brake disc casing to tap the inlet and outlet pressure between the disc blades in radial direction. This experimental rig can be tested using various brake disc specimen with constant outer diameter. The maximum revolution is up to 2600 rpm which is equivalent to 320km/h road speed.

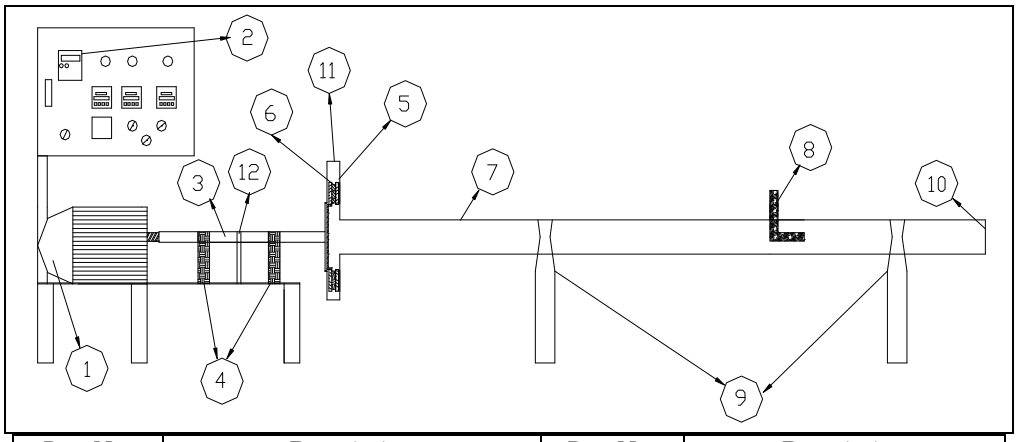

Part No.	Description	Part No.	Description
1	Single Phase Motor	7	Inflow Ducting
2	Motor Speed Controller	8	Pitot-tube Manometer
3	Connecting Shaft	9	Ducting Support
4	Bearing	10	Inflow
5	Disc Brake Casing	11	Outflow
6	Ventilated brake disc specimen	12	Magnetic speed pick-up

Figure 3: Schematic of experimental rig and the main components

3.1 Flow Measurements

The experimental rig is mainly developed to measure the amount air is metered into the ventilated brake disc and the pressure between the rotating blades. The inlet velocity is measured in the by taking the velocity integral in the inlet ducting. The screen which keeps the flow attached in a ducting is not needed because there is no sudden change in the diameter of the ducting, Mehta, [14]. Then, the entrance length, l_e was calculated with reference to Munson et. al. [15].

$$\frac{l_e}{D} = 0.06R_e \tag{1}$$

$$\frac{l_e}{D} = 4.4R_e^{\frac{1}{6}} \tag{2}$$

The equation (1) is for laminar flow and equation (2) is for turbulent flow. The lowest Reynolds Number, corresponding to the lowest value of inlet velocity was found to be 9273, which confirms that the flow is turbulent. Thus, equation (2) is used to calculate the entrance length. The entrance length l_e is calculated to be 2.1m for highest Reynolds number of 50,000. Thus, a 2.5m ducting is constructed for the pitot-static tube velocity measurement.

Figure 4 shows the pitot-static tube. The velocity of the free stream is calculated by the equation (3) below. The velocity in traverse direction as in Figure 5 is measured using pitot tube with reference to the BS1042. Then, the flow rate is calculated using multiple-application trapezoidal rule. An incline liquid manometer is used to measure the small static pressure difference.

$$V = \sqrt{2\frac{P_3 - P_4}{\rho}} \tag{3}$$

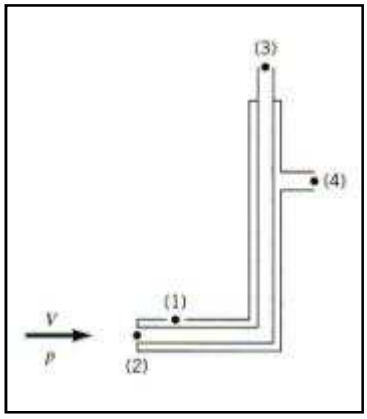

Figure 4: Pitot-Static tube

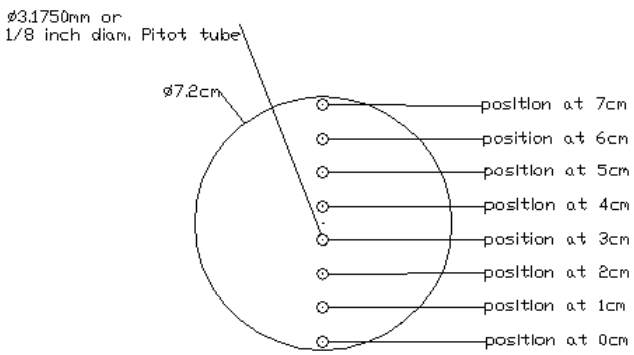

Figure 5: Traversed Pitot tube positioning at 8 radial points in pipe cross-section

4.0 EXPERIMENTAL RESULTS & UNCERTAINTY ANALYSIS

It is imperative that the flow measurements include the error analysis in order for it to be confidently compared with the CFD simulations. This forms the basis for the justification in using the CFD method for further analysis of streamlined brake discs.

Once the random and systematic errors in the experiment identified, they can be combined into an overall uncertainty of the measurement system. The usage of pitot-static tube to measure the velocity of incoming air flow need a detailed uncertainty analysis in order to reduce the error propagation in the experiment. The concept of repetition and random uncertainty are applied in the first stage of the measurement. The repetition method was used to reduce the random uncertainty associated with the fluctuation of readings. The already developed statistical concepts were used to analyze the repeated readings and to estimate the effect of random errors.

In the current work, a pitot-static tube was mounted traversely as in Figure 5 at different radial positions in a given cross-section of the pipe to measure the air flow velocity. The stagnation and static pressure ports were connected to an inclined manometer with and 5º inclination angles, having an accuracy of ±0.25% in the readings. The pressure value from the manometer reading is used to obtain the velocity of the air flow equation 3. An extensive calculation for the experimental errors is described in the Appendix.

Table 1 shows the summary of all the variables needed to obtain the volumetric flow rate, $\dot{Q}$ and error, $\sigma_{\dot{Q}}$ for discharge of air at straight blade disc rotating at 643 rpm. Table 2 shows the variation of total mass flow rate and error at different speeds for the straight blade brake disc.

Table 1: Volumetric flow rate and error for disc brake rotating at 643.06 rpm, straight blade disc

Radial position	V_{avrg} (m/s)	σ_v^+ (m/s)	σ_v^- (m/s)	V_{symm} (m/s)	σ_{symm} or Uv (m/s)	A (m^2)	σ_A (m^2)	$\dot{Q}$ (m^3/s)	$\sigma_{\dot{Q}}$ (m^3/s)	$\dot{Q}_{error}$ (%)
0	2.1400	0.3618	0.4238	2.1091	0.3928	0.000311	5E-07	0.000655	0.000122	18.6
1	2.5724	0.3498	0.2959	2.5993	0.3229	0.000250	5E-07	0.000650	8.07E-05	12.4
2	2.6177	0.2627	0.2279	2.6351	0.2453	0.000150	4E-07	0.000395	3.68E-05	9.32
3	2.8844	0.2096	0.1934	2.8925	0.2015	0.000150	4E-07	0.000434	3.03E-05	6.98
4	2.9596	0.2956	0.3020	2.9563	0.2988	0.000150	4E-07	0.000443	4.48E-05	10.1
5	2.5742	0.2373	0.2632	2.5613	0.2503	0.000150	4E-07	0.000384	3.76E-05	9.79
6	2.4855	0.2172	0.2619	2.4631	0.2396	0.000250	5E-07	0.000616	5.99E-05	9.72
7	2.2947	0.2986	0.3585	2.2648	0.3285	0.000311	5E-07	0.000703	0.000102	14.5

Table 2: Total mass flow rate and error for disc brake at different speed for straight blade brake disc

Speed (rpm)	Total mass flow rate, $\dot{m}$ (kg/s)	Error of $\dot{m}$, $\sigma_{\dot{m}}$(kg/s)	Percentage error of $\dot{m}$(%)
643.06	0.015736	0.000772	4.91
803.82	0.018476	0.000768	4.89
964.58	0.021109	0.000904	4.28
1125.35	0.024949	0.000740	2.97
1286.11	0.028033	0.000621	2.22
1446.88	0.030587	0.000630	2.06
1607.64	0.034655	0.000684	1.97
1800.00	0.040169	0.000698	1.74
2000.00	0.042714	0.000703	1.65

The measured inflow velocities for all rotational speeds are shown in Figure 6. As depicted, the curves in the Figure are not symmetric at the center line and the error bars intervals are noticeable, showing the effect of blockage bias.

In Figure 6, similar velocity profiles can be seen for the rotational speeds of 803 rpm and 946 rpm. The velocity curve is rather smooth but still not symmetric at the center line for 1125 rpm, which shows the blockage bias for higher but moderate speed. However, the error bars for this curve is smaller compared to the curves for the lower speeds, indicating that the blockage bias exist because of the use of Pitot tube but the effect is less due to the higher flow velocity. The curves for speed 1607 rpm, 1800 rpm and 2000 rpm are experiencing the same blockage bias, but the curve is not smooth. However, the error bars intervals are very small compared to previous curves.

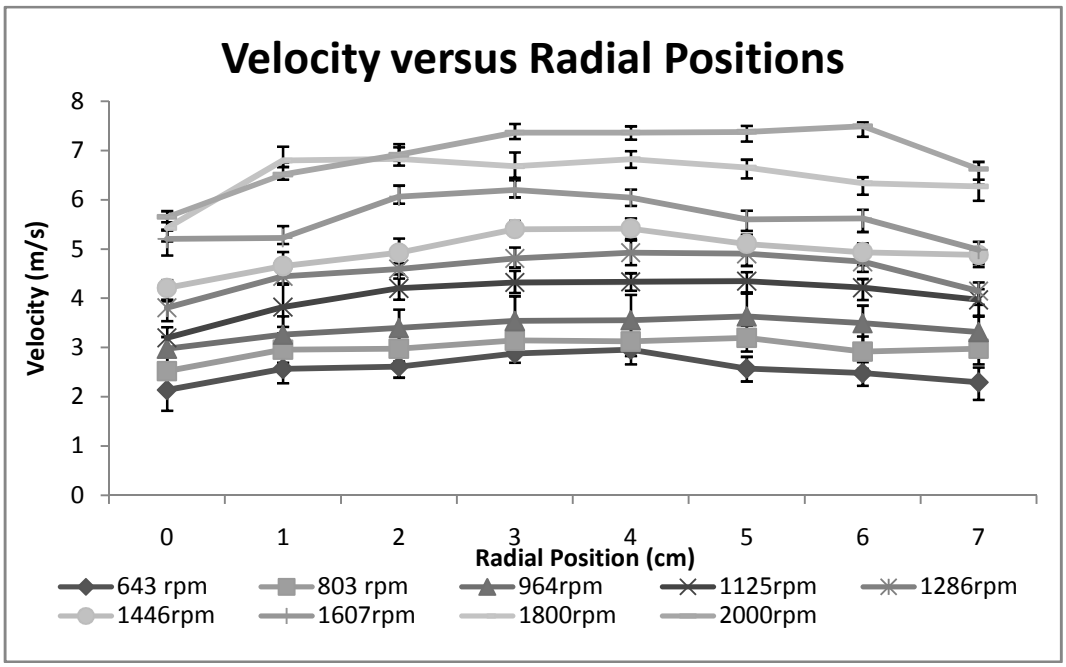

Figure 6: Traverse velocity result for different rotational speeds

Figure 7 shows the mass flow rate variation with increasing rotational speed. It should be noted that the error related to mass flow rate is comparatively low.

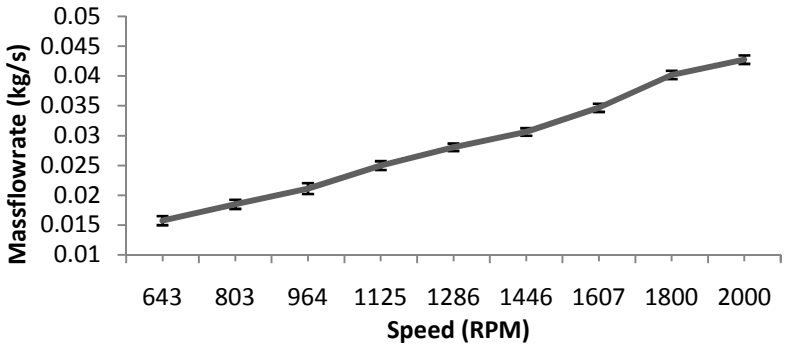

Figure 7: Mass flow rate for different rotational speeds

5.0 CFD SIMULATION OF FLOW THROUGH STRAIGHT BLADE VENTILATED DISC AND COMPARISON WITH EXPERIMENTAL RESULTS.

The extensive measurement of flow velocity completed in the experimental analysis is then used as boundary conditions to CFD analysis. The commercial CFD software FLUENT^{TM} is used.

The flow is periodical in the circumferential direction, thus only 1/36th of the geometry is modeled. Figure 8 shows the computational model generated and the appropriate boundary conditions applied for the current problem. The model consists of 355,000 mesh, comprising of tetrahedral and hexahedral elements. A grid dependency study was carried out and the optimal numbers of grid points which gave a satisfactory compromise between accuracy and computational time are chosen.

RNG k-ε two-equation model is selected for the turbulence transport equations and standard wall treatment available in FLUENT^{TM} Segregated solver was chosen since the flow is relatively low speed and the pressure correction method is used for the flow field calculation. The computational model is then simulated for various rotational speeds with reference to the experimental configurations until the residual error is less than 10^{-5}. The 3-dimensional computational results then post processed to extract pressure point data to compare with the blade inlet pressure experimental data.

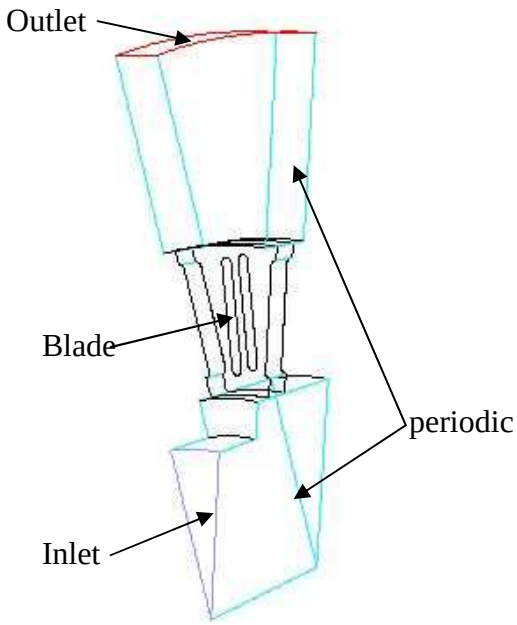

Figure 8: CFD Boundary conditions for straight blade ventilated brake disc

Figure 9 shows the comparison between inlet pressure values obtained from CFD with the measured values from experiment. The trend shows that the inlet pressure reduces as the rotational speed increases. Some discrepancies can be seen in Figure 9; for the first two rotational speeds the differences are less than 5% and the next 3 speeds the differences are around 7%. The discrepancy at high rotational speeds could be due to the highly swirling flow and thicker boundary layer developed in the real case.

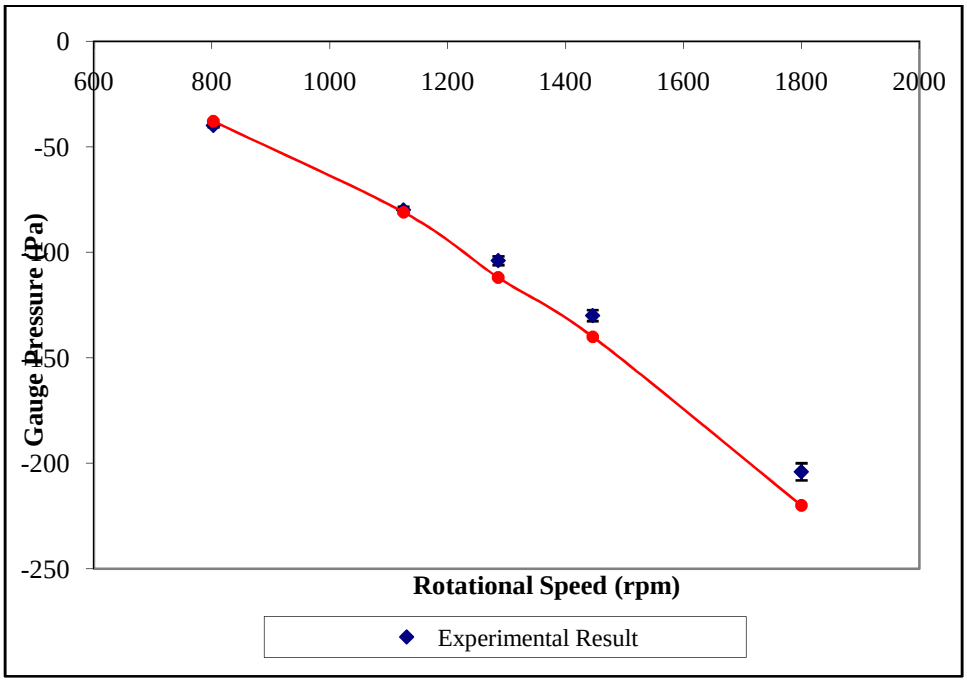

Figure 9: Comparison of simulation results against experimental for blade inlet pressure.

6.0 BLADE TILTING IMPROVEMENT TO STRAIGHT BLADE CONFIGURATION

The CFD simulation is completed with converged results. The mass flow results are tabulated below in Table 3. The percentage improvement is ranging from 30% to 48%. The higher rotational speed has higher magnitude of improvement. The same results are also presented in graphical manner as in Figure 10. The trend of both brake discs is linear. Figure 11 till Figure 14 shows the velocity distribution of the baseline and the 30º tilted angle blade disc. The velocity is higher the leading edge of the tilted disc. Higher pumping effect is noticed in the titled velocity distribution. Figure 15 below illustrates the CFD results of velocity vector distribution at mid-plane view of the brake disc. The baseline results show a major recirculation at the pressure side near the trailing edge. However, the velocity vector plot for 30º tilted disc has eliminated the re-circulation. Thus the higher amount air can be metered through the flow passage of the improved disc brake.

Table 3: Mass flow comparison between staright blade (baseline) and 30º titled angled blade

Speed (RPM	Baseline (g/s)	30º angled blade (g/s)	% Improvement
643	5.23	6.75	29
804	6.91	8.95	29
1125	10.14	12.46	23
1286	11.23	14.37	28
1447	12.37	16.03	30
1608	13.46	18.00	34
1800	14.47	20.08	39
1929	15.30	21.80	42
2089	16.50	23.70	44
2250	17.60	25.60	45
2411	18.70	27.60	48
2572	19.90	29.40	48

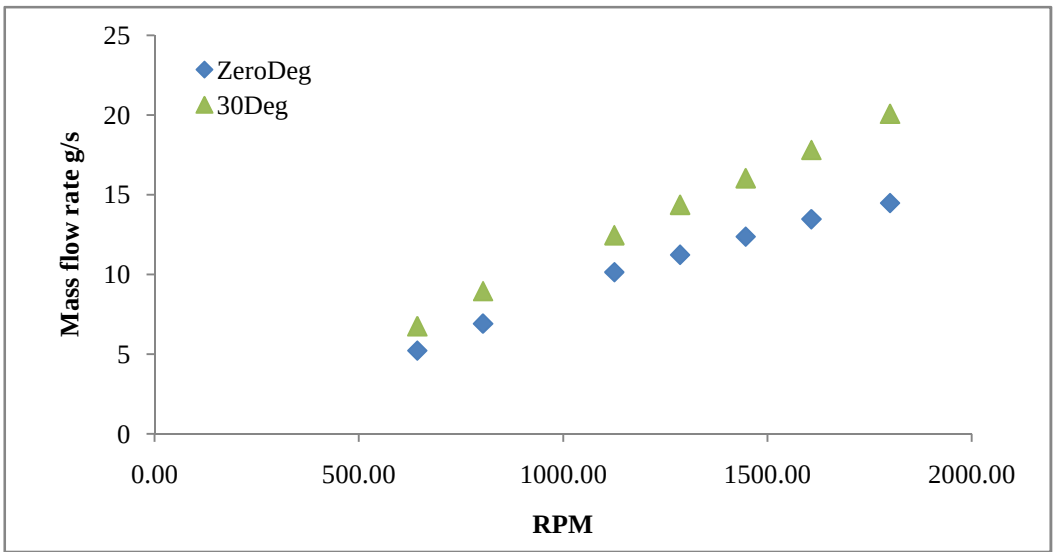

Figure 10 : Mass flow rate against rotational speed

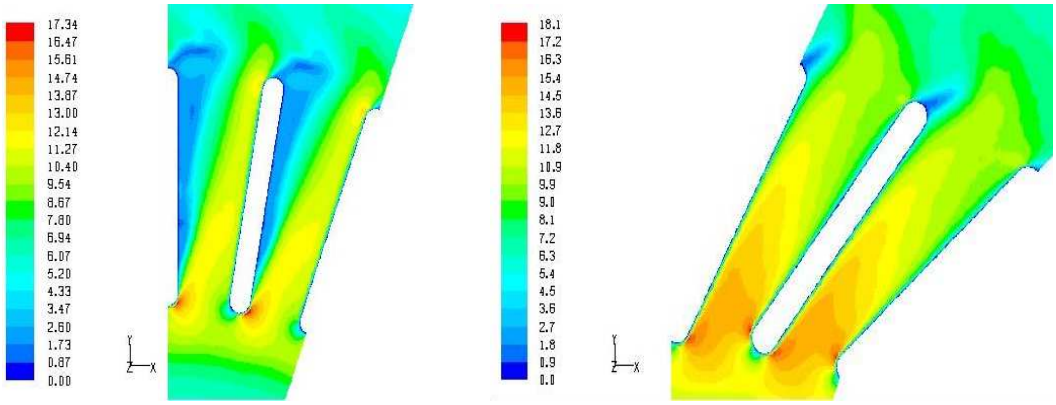

(a) Baseline (0°) (b) 30°

Figure 11: Velocity contour plot for inclined brake disk design at 803 rpm

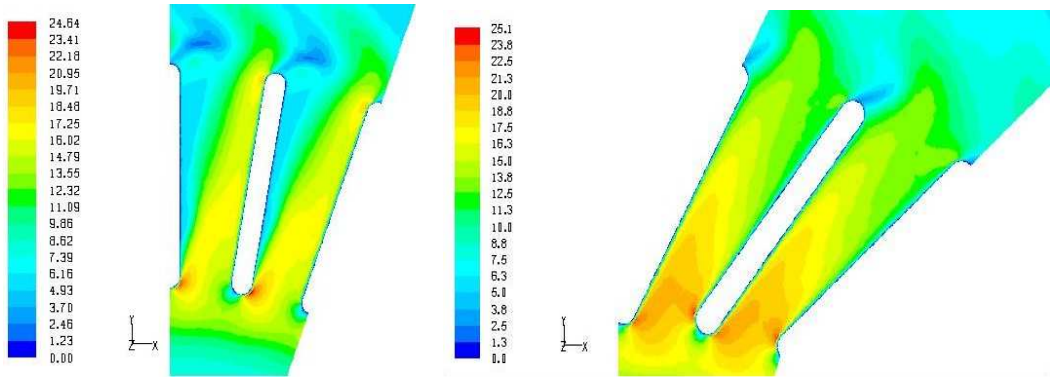

(a) Baseline (0°) (b) 30°

Figure 12 : Velocity contour plot for inclined brake disk design at 1125 rpm

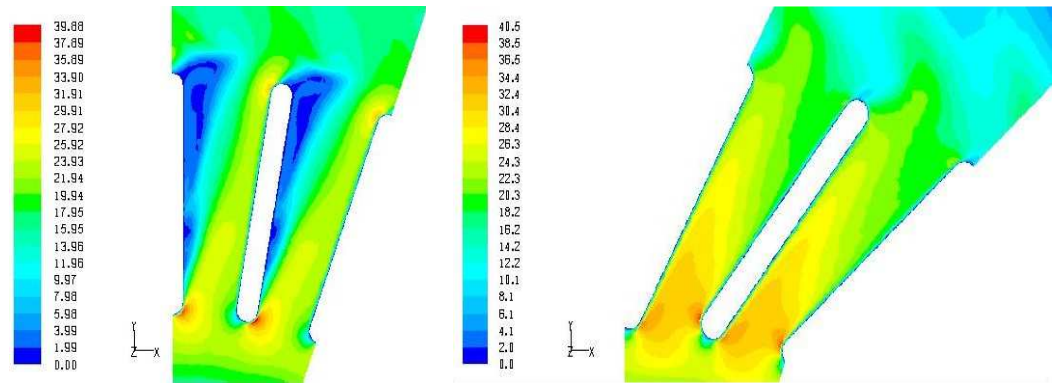

(a) Baseline (0°) (b) 30°

Figure 13 : Velocity contour plot for inclined brake disk design at 1800 rpm

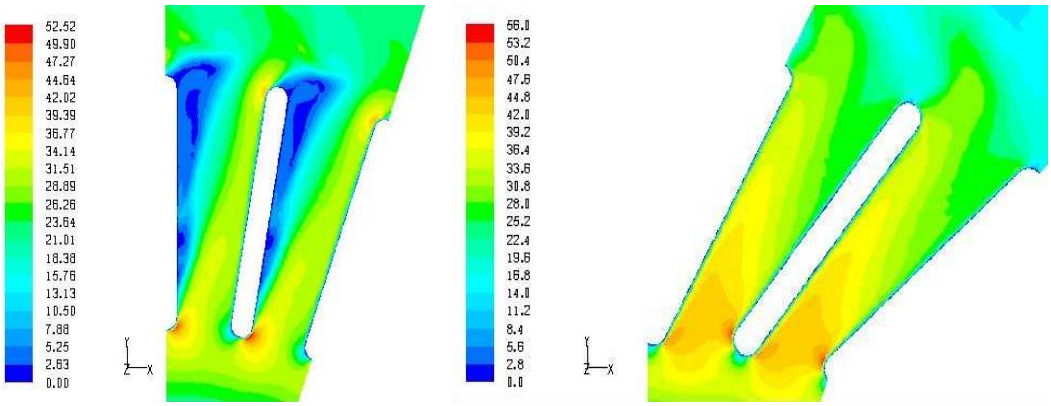

(a) Baseline (0°) (b) 30°

Figure 14 : Velocity contour plot for inclined brake disk design at 2411 rpm

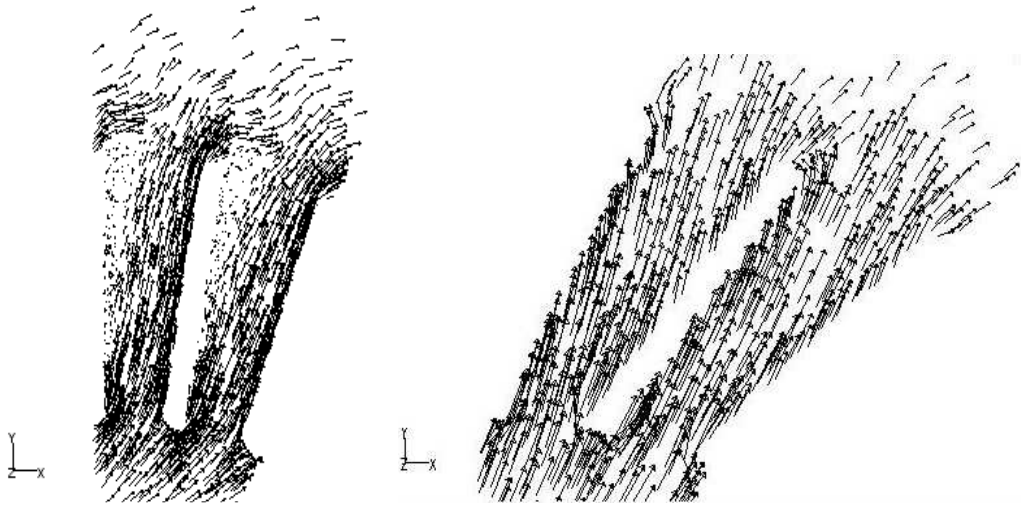

(a) Baseline (0°) (b) 30°

Figure 15 : Velocity vector plot for inclined brake disk design at 1125 rpm

7.0 CONCLUSION

The current work shows that simple tilting of the ventilated disc blade can have a significant improvement on mass flow. Titling the blade in the right direction has reduced the flow incidence angle, thus eliminated re-circulation in the passage flow. The improvement is very encouraging while the advantage of bi-directional characteristics of baseline disc has to be compromised.

ACKNOWLEDGEMENT

The author would like to acknowledge the Ministry of Science, Technology and Innovation of Malaysia (MOSTI) and Universiti Tenaga Nasional for the financial support for this project.

REFERENCES

1. Newcomb, T.P. and El-Sherbiny, M., *Liquid-cooled disc brake.* 1975, Wear , pp. 311-317.
2. Dow, T. A. *Thermoelastic effects in brakes* wear, 1980, Vol. 59.
3. Moore, D. F.*Design of a prototype braking simulator.* IPC Business Press: TRIBOLOGY International, 1980.
4. Yevtushenko, A. and Ivanyk, E. *Determination of heat and thermal distortion in braking systems.* Proceedings of Wear, 1995, Vol. 185, pp. 159-165.
5. Laskaj, Matthew and Benjamin, Murphy, *Improving the efficiency of cooling the front disc brake on V8 racing car.*. Melbourne, 1999.
6. Harmand, S., Watel, B. and Desmet, B. *Local convective heat exchanges from a rotor facing a stator.* Int. journal thermal science, 1999, Vol. 39, pp. 404-413.
7. Johnson, D. A., Sperandei, B. A. and Gilbert, R. *Analysis of the flow through a vented automotive brake rotor.* Journal of fluid engineering, 2003, Vol. 125, pp. 979-986.
8. Panier, S., Dufreney, P. and Weichert, D. *An experimental of hot spots in railway disc brakes.* Proceedings of Wear, 2004, Vol. 257, pp. 687-695.
9. Vernersson, T. *Thermally induced roughness of tread-braked railway wheels part 1: brake rig experiments.* Proceedings of Wear, 1999, Vol. 236, pp. 96-105.
10. Cunefare, K. A. and Graf, A. J. *Experimental active control of automotive disc brake rotor sequeal using dither.*: Journal of sound and vibration, 2002, Vol. 250, pp. 579-590.
11. Sherif, H. A. *Investigation on effect of surface topography of pad/disc assembly on sequeal generation.*: Proceedings of Wear, 2004, Vol. 257, pp. 687-695.
12. Desplanques, Yannick, et al. *Analysis of tribological behaviour of pad-disc contact in railway braking Part 1: Laboratory test development, comprises between actual and simulated tribological triplets.* Proceedings of Wear, 2006, Vol. 262, pp. 582-591.
13. Uyyuru, R. K., Surappa, M.K. and Brusethaug, S. Bangalore, *Tribological behaviour of Al-Si-SiCp composites/autmobile brake pad system under dry sliding conditions* 2007, Tribology International, Vol. 40, pp. 365-373.
14. Mehta, R. D. and Bradshaw, P. *Technical notes, design rules for small low speed wind tunnels.* The aeronautical journal of the royal aeronautical society, 1979, pp. 443-449.
15. Munsun, B. R., Young, D. F. and Okishi, T. H. *Fundamentals of fluid mechanics* John Wiley & Sons Inc, 1998.